AFRL-RY-HS-TR-2011-0017

Development of RF Sensor Based on Two-Cell Squid

Fengbin Song, Ming He, and Alexey Ustinov
Physikalisches Institut
Karlsruhe Institute of Technology
Karlsruhe, Germany

15 July 2011

Final Report

AIR FORCE RESEARCH LABORATORY
Sensors Directorate
Electromagnetics Technology Division
80 Scott Drive
Hanscom AFB MA 01731-2909

NOTICE AND SIGNATURE PAGE

This report was cleared for public release by the Electronic Systems Center Public Affairs Office for the Air Force Research Laboratory, Electromagnetics Technology Division and is available to the general public, including foreign nationals. Copies of this report may be obtained from the Defense Technical Information Center (DTIC) (http://www.dtic.mil).

AFRL-RY-HS-TR-2011-0017 HAS BEEN REVIEWED AND IS APPROVED FOR PUBLICATION IN ACCORDANCE WITH ASSIGNED DISTRIBUTION STATEMENT.

STANFORD P. YUKON
Senior Physicist
Electromagnetic Scattering Branch

BERTUS WEIJERS
Branch Chief
Electromagnetic Scattering Branch

ROBERT V. MCGAHAN
Technical Communication Advisor
Electromagnetics Technology Division

This report is published in the interest of scientific and technical information exchange, and its publication does not constitute the Government's approval or disapproval of its ideas or findings.

REPORT DOCUMENTATION PAGE

The public reporting burden for this collection of information is estimated to average 1 hour per response, including the time for reviewing instructions, searching existing data sources, gathering and maintaining the data needed, and completing and reviewing the collection of information. Send comments regarding this burden estimate or any other aspect of this collection of information, including suggestions for reducing the burden, to Department of Defense, Washington Headquarters Services, Directorate for Information Operations and Reports (0704-0188), 1215 Jefferson Davis Highway, Suite 1204, Arlington, VA 22202-4302. Respondents should be aware that notwithstanding any other provision of law, no person shall be subject to any penalty for failing to comply with a collection of information if it does not display a currently valid OMB control number.
PLEASE DO NOT RETURN YOUR FORM TO THE ABOVE ADDRESS.

1. REPORT DATE *(DD-MM-YYYY)*	2. REPORT TYPE	3. DATES COVERED *(From - To)*

4. TITLE AND SUBTITLE

5a. CONTRACT NUMBER

5b. GRANT NUMBER

5c. PROGRAM ELEMENT NUMBER

6. AUTHOR(S)

5d. PROJECT NUMBER

5e. TASK NUMBER

5f. WORK UNIT NUMBER

7. PERFORMING ORGANIZATION NAME(S) AND ADDRESS(ES)

8. PERFORMING ORGANIZATION REPORT NUMBER

9. SPONSORING/MONITORING AGENCY NAME(S) AND ADDRESS(ES)

10. SPONSOR/MONITOR'S ACRONYM(S)

11. SPONSOR/MONITOR'S REPORT NUMBER(S)

12. DISTRIBUTION/AVAILABILITY STATEMENT

13. SUPPLEMENTARY NOTES

14. ABSTRACT

15. SUBJECT TERMS

16. SECURITY CLASSIFICATION OF:			17. LIMITATION OF ABSTRACT	18. NUMBER OF PAGES	19a. NAME OF RESPONSIBLE PERSON
a. REPORT	b. ABSTRACT	c. THIS PAGE			
					19b. TELEPHONE NUMBER *(Include area code)*

TABLE OF CONTENTS   PAGE

LIST OF FIGURES   PAGE

ABSTRACT

The RF directional sensor based on phase-sensitive detection using two sorts of Josephson parametric amplifiers has been analyzed and investigated experimentally. To construct the Josephson parametric amplifier, we use a SQUID (either single-cell SQUID or two-cell SQUID) embedded in a superconducting coplanar waveguide. We operated the circuit at a frequency of several GHz and measured the amplitude response of the SQUID-based Josephson parametric amplifier. Nonlinearity and flux tunability in the reported experiments was limited by relatively large critical current density and therefore small nonlinear inductance of the SQUID. The demonstrated phase sensitivity was 1.2 dB / rad. It appears feasible to improve the sensitivity of developed RF sensor by reducing the critical current of the Josephson junctions.

Introduction

The Superconducting Quantum Interference Device (SQUID), a superconducting loop interrupted by two Josephson junctions, is an extremely sensitive detector of magnetic flux, and has been used in a wide variety of applications for almost for half a century. However, limited by the local heating and relaxation time of the SQUID and operation frequencies of readout circuits, the conventional SQUIDs mostly work at frequencies below 1 GHz [1-2]. Alternatively, the SQUID can be considered as flux-modulated nonlinear inductor L_J, determined by the critical current I_0 and the phase difference φ of the Josephson junction. Based on this unique character, various parametric amplifiers have been demonstrated [3-10], with sensitive response to RF signals, especially for the phase of the signal. Recently, the SQUIDs were embedded into superconductive Coplanar Waveguide Resonators (CWRs), which provided controllable and low-noise microwave surroundings [11-12] and allowed the construction of Josephson parametric amplifiers working at GHz frequencies [9, 13, 6, 5].

In this report, we present rather promising investigations of RF directional sensors operated in two different regimes, namely as the phase-shift sensitive Josephson bifurcation amplifier (PJBA) and the amplitude-response Josephson parametric amplifier (AJPA).

The idealized model of the proposed RF directional sensor is illustrated in Fig. 1. The phase difference δ of the RF signals received by two spatially separated detectors can be written as

$$\delta = \frac{2\pi d \sin\theta}{\lambda}$$

where θ denotes the angle of the incoming RF signal, d is the distance between the two detectors and λ the wavelength of the RF signal. Therefore the RF phase-sensitive measurement is essential for the directional sensitivity.
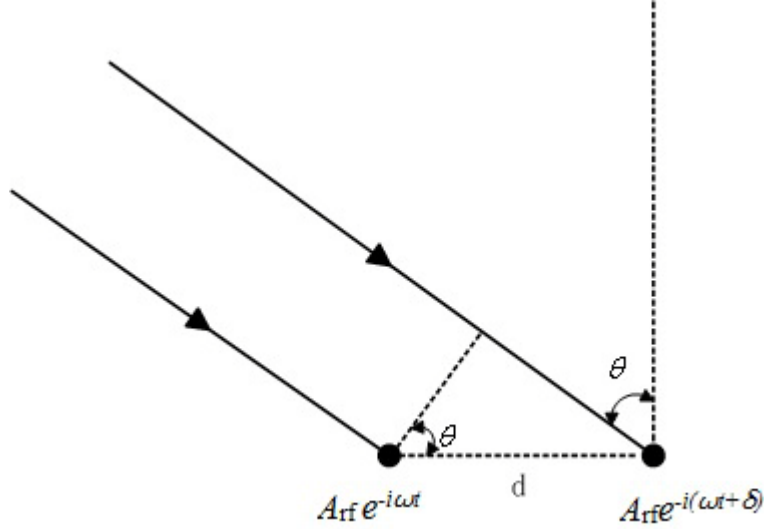
Figure 1. The idea of the RF directional sensing.

1. Theory

Various parametric amplifiers based on Josephson junctions have been recently extensively investigated. With near quantum limited performance, the parametric amplifiers were successfully utilized as readouts of the superconducting qubits [7, 9]. Small variations in the junction critical current I_0 can significantly change the transmission through the junction under appropriate bias conditions. Therefore, an external signal such as magnetic flux or RF radiation, which could influence the parameter I_0, will be effectively amplified. This is the reason why they are named as the parametric amplifiers. For both PJBA and AJPA, we embedded SQUIDs in the centre line of CWRs, which provided well-defined electromagnetic surrounding at high frequencies.

1.1 The phase-shift based Josephson bifurcation amplifier (PJBA)

Let us consider a Josephson junction embedded in a half-wave CWR as shown in Fig. 2(a). This junction can be also represented by a SQUID with the critical current given by $I_c(\Phi) = 2I_0 |\cos(\pi\Phi/\Phi_0)|$, where Φ is the flux through the SQUID loop and Φ_0 is the magnetic-flux quantum. Thus the SQUID can be treated as a junction with a flux-dependent critical current. Once one makes a single mode approximation for the CWR near its resonant frequency ω_0, one arrives at the equivalent LCR circuit shown in Fig. 2(b) [7].
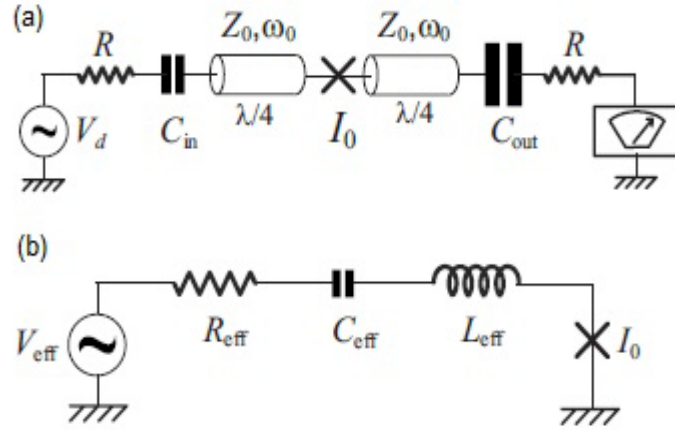
Figure 2. (a) Circuit diagram of the half-wave CWR with a Josephson junction in the middle.

(b) The corresponding equivalent LCR circuit.

The effective inductance and capacitance of this circuit are $L_{eff} = \pi Z_0/2\omega_0$ and $C_{eff} = 2/(\pi Z_0\omega_0)$, where the Z_0 is the characteristic impedance of the transmission line of the CWR. In our case, the fundamental mode resonant frequency of the CWR $\omega_0/2\pi$ was around 9.6 GHz. The quality factor Q of the CWR is

$$Q = 1/\omega_0 R_{eff} C_{eff} \tag{1}$$

and therefore

$$R_{eff} = 1/\omega_0 Q C_{eff} \tag{2}$$

With Kirchoff's law, the dynamics of the equivalent circuit near ω_0 can be expressed as follows:

$$L_{eff}\ddot{q}(t) + R_{eff}\dot{q}(t) + q(t)/C_{eff} + (\Phi_0/2\pi)\dot{\varphi}(t) = V_d\cos(\omega_d t) + V_N(t) \tag{3}$$

where ω_d is the drive frequency, q is the charge on the capacitor C_{eff} and $V_N(t)$ is the effective thermal noise of the impedance R_{eff}. Considering the Josephson relations:

$$I(t) = I_c\sin\varphi(t)$$
$$V(t) = \frac{\Phi_0}{2\pi}\dot{\varphi}(t) \tag{4}$$

the Josephson nonlinear inductance is

$$L_J = \frac{\Phi_0}{2\pi I_c\cos(\varphi)} \tag{5}$$

For the equation (3), we therefore obtain:

$$(L_{eff} + \Phi_0/2\pi I_c\sqrt{1 - \dot{q}(t)^2/I_0^2})\ddot{q}(t) + R_{eff}\dot{q}(t) + q(t)/C_{eff} = V_d\cos(\omega t) + V_N(t) \tag{6}$$

If we assume harmonic solutions for $q(t)$ at the drive frequency ω_d of the form $y(t)exp(i\omega_d t)$ + c.c., one can show that the equation of motion for the dimensionless slowly varying complex amplitude $u(\tau)$ corresponding to Eq. (6) can be reduced to

$$\frac{du}{d\tau} = -\frac{u}{\Omega} - iu(|u|^2 - 1) - i\sqrt{\beta} + f_N(\tau) \tag{7}$$

where

$$\Omega = 2Q(1 - \omega_d/\omega_{p0}) \tag{8}$$

$$\omega_{p0} = \sqrt{\frac{1}{(L_{eff} + \Phi_0/2\pi I_c)C_{eff}}} \tag{9}$$

$$u = \sqrt{\frac{1}{2\Omega\varepsilon^2}}\frac{\omega_d}{I_c}y \tag{10}$$

$$\beta = \frac{V_{rf}^2}{(\Phi_0/2\pi)^2\omega_d^2}(1/2\Omega\varepsilon^2)^3 \tag{11}$$

$$\varepsilon = \sqrt{(1 + 2\pi L_{eff}I_c/\Phi_0)/Q} \tag{12}$$

where Ω according to (8) is proportional to the reduced drive detuning, ω_{p0} is the resonant frequency for small oscillations, i.e. the plasma frequency of the combined system, $\tau = (\omega_{p0} - \omega_d)t$ is the dimensionless slow time, β is the reduced drive power, and $f_N(\tau)$ is the reduced noise term. Actually, the Eq. (7) has been derived under the rotating wave approximation with only leading order nonlinear terms being retained in Eq.(6) [7]. In this case, the equivalent circuit behaves like a Duffing oscillator.
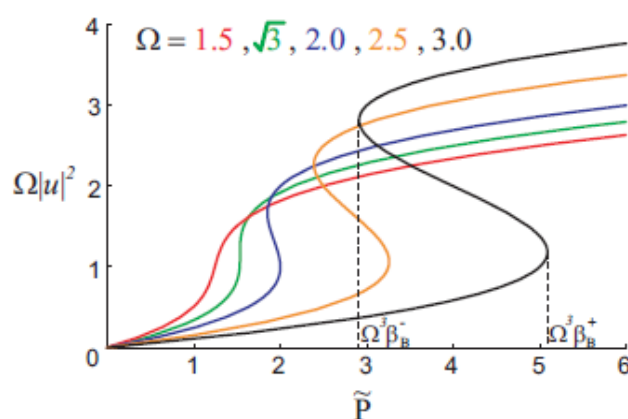
Figure 3. Steady state solutions of Eq. (7) for increasing (left to right) values of reduced detuning Ω [7]. The magnitude squared of reduced oscillation amplitude $\Omega|u|^2$ is plotted as a function of reduced drive power $\widetilde{P} = \Omega^3\beta$.

And the steady state solutions of Eq. (7) can be obtained with $du/d\tau = 0$. For a given drive frequency ω_d such that $\Omega > \sqrt{3}$, the system exhibits bi-stability when the drive power is large enough, as shown in Fig. 3.

In our case, since the β_L of the SQUID was around 1, the flux-dependent critical current should be 17.7 µA$< I_c <$ 35.4 µA, and thus 9.528 GHz $< \omega_{p0}/2\pi <$ 9.564 GHz. For the drive frequency ω_d around 9.55 GHz and the quality factor $Q = 700$, we could in principle obtain $\Omega > \sqrt{3}$ in some range of drive power. However, in fact another essential condition to reach the very sensitive and therefore attractive bifurcation regime is that the current through the junction I_B must be lower that I_c:

$$I_B = \frac{4I_c}{\sqrt[4]{3}} \sqrt{\frac{L_{eff} + L_J}{L_J Q}} < I_c \tag{13}$$

For our parameters with fabricated samples (see below), we obtain 1.316 $< I_B / I_c <$ 1.320. Therefore, being limited by the relatively low Josephson inductance L_J and the quality factor Q, we could not reach the bifurcation regime with our present samples. Even so, it was still possible for us to reach the nonlinear regime which is just below the bifurcation regime (shown in Fig. 4a). In this nonlinear regime, the resonant frequency of CWR combined with the SQUID ω_s would shift to lower frequencies with increasing the drive power, and the resonator could serve as one sort of conventional parametric amplifiers (the PJBA) [9].
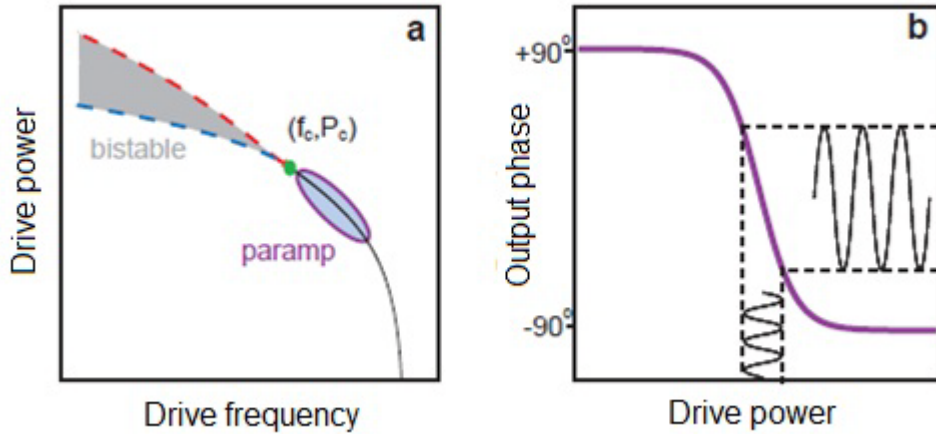
Figure 4. The phase diagram [9] of the amplifier resonator is shown schematically in (a). The resonance frequency (solid line) gradually decreases with increasing drive power. Above a critical drive power P_C and below a critical frequency f_C the resonator is bistable. At powers slightly below P_C, the resonator functions as a conventional parametric amplifier (paramp). (b) shows a line cut of (a) at constant drive frequency in this nonlinear regime. A weak signal modulating the drive power leads to large changes in the phase of the output response.

As shown in Fig. 4b, a weak pump signal at the drive frequency is combined with the drive and modulated its amplitude, resulting in a large change in the phase of the

output response. Since only signals in phase with the drive will be amplified, the resonator behaves as a phase-sensitive amplifier. The signals which are 90 degrees out of phase with the drive do not affect the drive amplitude to first order and hence do not get amplified [9]. In other words, the pump signal in phase with the drive can effectively influence the combined drive power and thus change the resonant frequency ω_s. If we observe the phase of output response of the CWR at fixed frequency in the nonlinear regime, it should shift with the amplitude and the phase of the pump signal.

1.2 The amplitude-response based Josephson parametric amplifier (AJPA)

We also studied AJPA, which provides amplitude response to the phase difference δ of RF signals. The demonstration of this parametric amplifiers was first implemented with dc biased Josephson junctions [14-15, 4], and then with SQUIDs embedded in CWRs [5] and, more recently, with superconducting transmission lines [6] .

For the parametric amplifier based on the dc biased junctions, the drive oscillation is provided by the AC Josephson oscillation as the junction biased at a fixed dc voltage. While for the one based on the embedded SQUIDs, the drive oscillation is inputted through the CWR or the transmission line. Due to the nonlinearity of Josephson inductance, under additional pump, mixed signals can be obtained at combined frequencies of ω_d, ω_p such as $\omega_p - \omega_d$, $\omega_p + \omega_d$, $2\omega_p - \omega_d$, and so on, where the ω_d is the drive frequency and the ω_p the pump frequency [15]. If the frequency of mixed signal ω_m is near to the resonant frequency of the combined circuit of parametric amplifier, the mixed signal will be efficiently amplified.

In our case, the ω_d was around the resonant frequency of combined CWR ω_s, and the $\omega_p = 2\omega_d$, hence the $\omega_m = \omega_p - \omega_d = \omega_d$ also around ω_s. Consequently, the mixed signal, which indicated the interaction of the drive and the pump, would be enhanced by the CWR.

Since both of the drive and the pump were coupled into the embedded SQUID with the magnetic field component. If the ω_d and ω_p obey

$$\max(\omega_d, \omega_p) << \min(\omega_{cut}, \omega_c) \tag{14}$$

$$\omega_{cut} = R_n / L \tag{15}$$

$$\omega_c = 2\pi R_n I_c / \Phi_0 \tag{16}$$

where R_n is the normal resistance of the Josephson junction in the SQUID, and L the inductance of the SQUID loop, the RF flux Φ_{rf} in the SQUID loop can be considered to be relatively static. In our case, the $\omega_{cut} / 2\pi$ was around 1820 GHz and $\omega_c / 2\pi$ about 948 GHz; while the $\omega_p / 2\pi = 2\omega_d / 2\pi$ was around 19 GHz. Therefore, the above condition applied, and the influence of the Φ_{rf} on I_c are discussed as follows.

For a single SQUID (shown in Fig. 5a) with no dc biased current through it, the circulating supercurrent in the loop is

$$I_s(t) = I_0 \sin \varphi_1 = -I_0 \sin \varphi_2 \qquad (17)$$

where I_0 is the critical current of each junction and φ_i the phase of each junction ($\varphi_1 = -\varphi_2$). If a RF-drive with frequency ω_d and a RF-pump with frequency ω_p apply on the SQUID, the phase difference of the two junctions is given by

$$\varphi_2 - \varphi_1 = \frac{2\pi}{\Phi_0}(\Phi_d \cos(\omega_d t + \theta_d) + \Phi_p \cos(\omega_p t + \theta_p) + LI_0 \sin \varphi_1) \qquad (18)$$

where Φ_d is the amplitude of the flux caused by the RF-drive and Φ_p is the amplitude of the flux caused by the RF-pump. If the L and the I_0 are relatively small, i.e. the component of Φ_{rf} induced by the $I_s(t)$ can be ignored, the Eq. (17) can be written as:

$$I_s(t) = -I_0 \sin\left[\frac{\pi}{\Phi_0}(\Phi_d \cos(\omega_d t + \theta_d) + \Phi_p \cos(\omega_p t + \theta_p))\right] \qquad (19)$$

which has the Fourier components spectrum[4]:

$$I_s(t) \propto -I_0 \sum_{-\infty}^{+\infty} J_n \sin\left[(\omega_p + n\omega_d)t + \theta_p + n\theta_d\right] \qquad (20)$$

For $\omega_p = 2\omega_d$ the Fourier component near ω_d is

$$I_0\left[J_1 \sin(\omega_d t + \theta_p - \theta_d) - J_3 \sin(\omega_d t - \theta_p + 3\theta_d)\right] \qquad (21)$$

Therefore, the component of the circulating current I_s at the frequency ω_d is related with the phase difference of the drive and the pump. The output amplitude of CWR at ω_d is proportional to the value of this component. In some cases, the output amplitude at ω_d can be smaller even under the pump, compared with the original amplitude caused only by the drive without the pump. This effect is usually named as deamplification [5-6], which by itself is a remarkable characteristics of the parametric amplifier.

2. Experiments

2.1 Samples
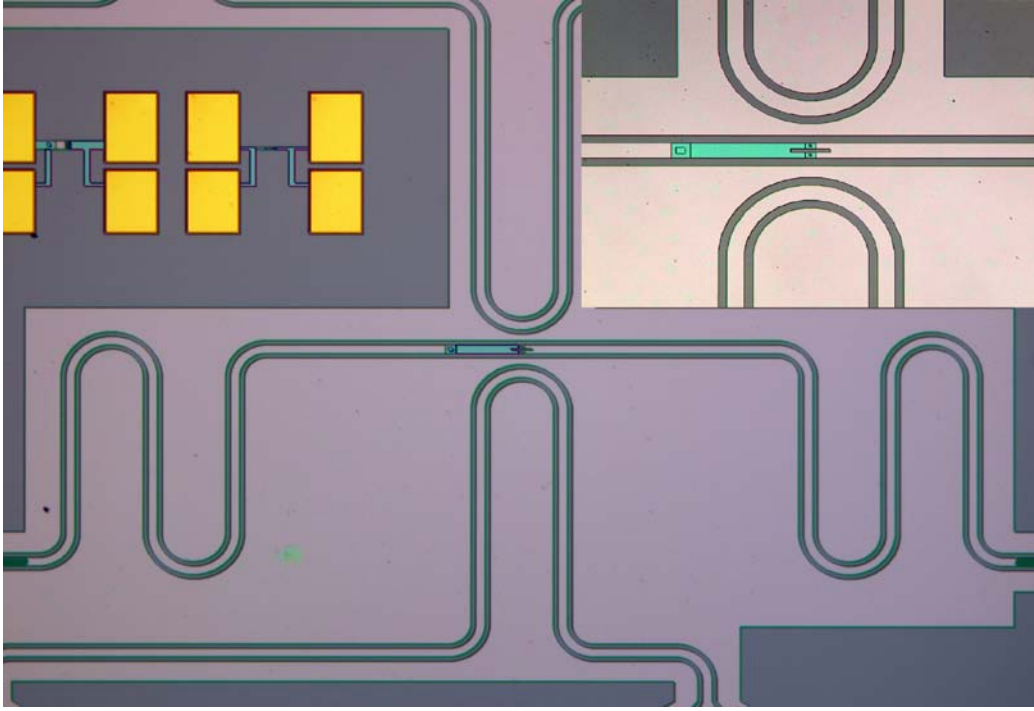
(a)
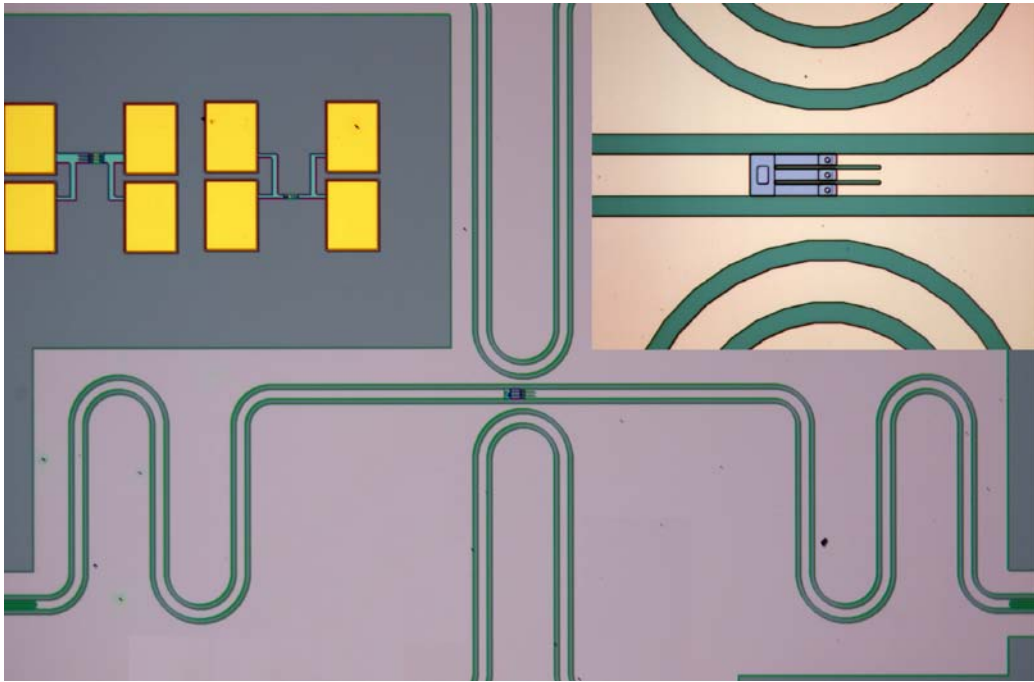
(b)

Figure 5. Micro-photographs of the studied samples. (a) The single SQUID sample: one SQUID embedded in the CWR; (b) The two-cell SQUID sample: a two-cell SQUID embedded in the CWR. For each sample, two coplanar coils were located on the both sides of the SQUID separately. The enlarged view of the SQUID is shown as an inset in the top right corner of each figure.

We investigated two samples with different designs. Both the single SQUID and the two-cell SQUID samples are included in this report and are shown in Fig. 5. The SQUID (single SQUID or two-cell SQUID) was embedded in the centre of the CWR, with designed resonant frequency ω_0 around 9.6 GHz and quality factor Q of about 700. Two coplanar coils were arranged on the both sides of the SQUID separately, which allowed us to apply static magnetic field and/or RF signal to the SQUID. The termination capacitors of the CWR (also shown in Fig.5) were about 9 fF. The critical current I_0 of each junction in the SQUID was 17.7 µA, normal resistance 110.9 Ω, plasma frequency ω_p 124 GHz and characteristic frequency 948 GHz. While the loop inductance of SQUID was 60 pH, and the corresponding β_L equals to 1.04.

2.2 Measurement setup

Our measurement setup is exhibited in Fig. 6. The drive RF signal was attenuated by 20 dB prior to the input port of the CWR on our sample. And the output response of the CWR was first isolated from external noise with -10 dB attenuator, transmitted through a band-pass filter and then amplified with low-temperature amplifier by +35 dB, before getting observed by a spectrum analyzer. In some measurements, to obtain transmission characteristics we used a network analyzer instead of the RF source and spectrum analyzer. The samples and cryogenically used devices next to them were immersed in liquid helium and protected from stray dc and magnetic fields by a cryoperm shield. The dc bias current for flux modulation and/or RF pumps were applied to the SQUIDs using the coplanar field lines.
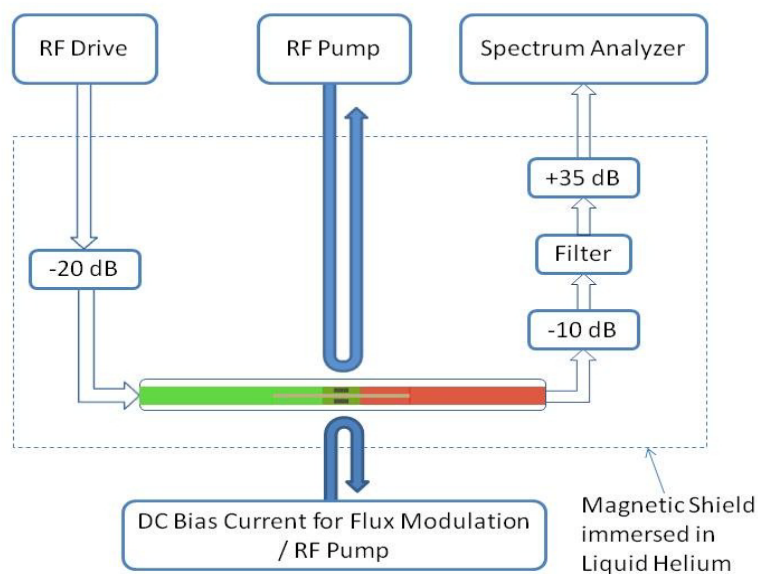
**Figure 6.** Schematic diagram of the measurement setup.

3. Measurements and discussion

Following the above theoretical consideration, our measurements focused on two

independent methods (PJBA and AJPA) to develop RF phase-sensitive sensors. Both the single SQUID sample and the two-cell SQUID sample were investigated.

3.1 Basic transmission response

Basic resonant response of CWR ω_s on the single SQUID sample (see Fig. 5(a)) under static flux modulation was first measured with a network analyzer, as shown in Fig. 7. The static flux modulation was applied by dc biased current through one of the coplanar coils on the sample. The resonant frequency $\omega_s / 2\pi$ was shifted from 9.557 GHz to 9.551 GHz by increasing the applied static flux Φ_a from zero to about 0.5 Φ_0.
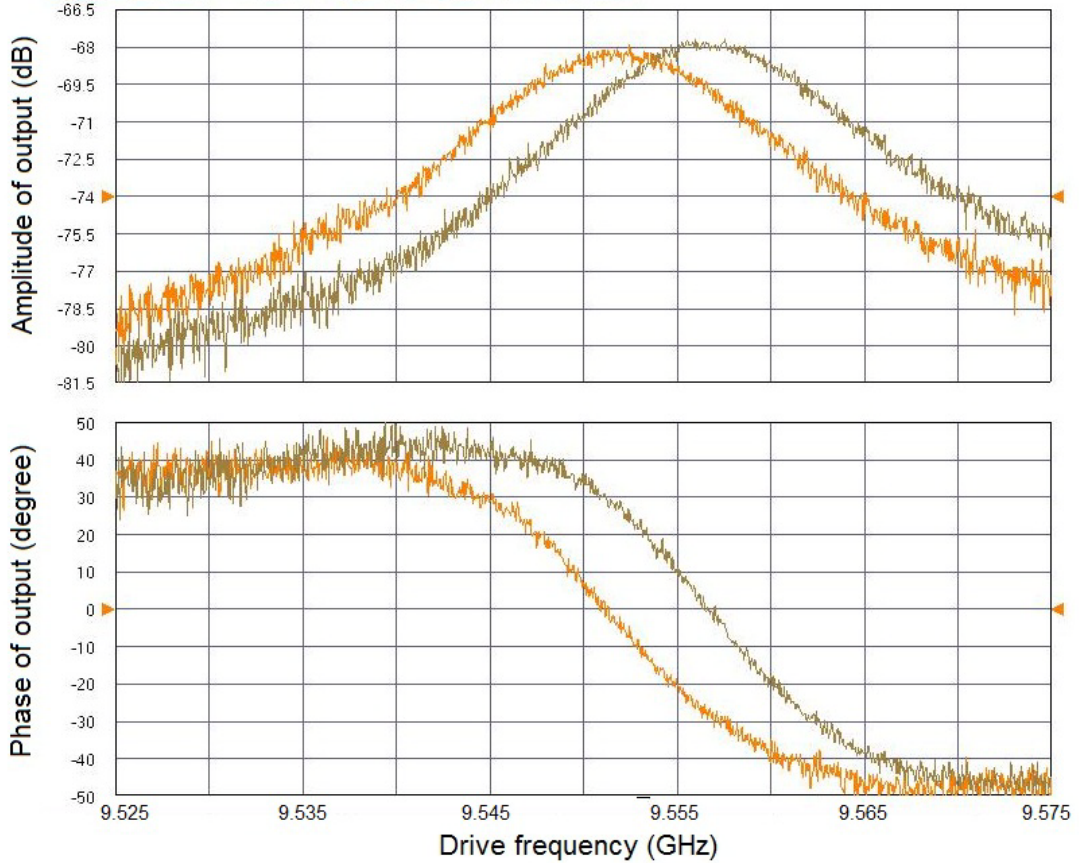
Figure 7. Resonant response including amplitude and phase of the CWR on the single SQUID sample with static flux modulation. The applied static flux is $\Phi_a = 0$ for the brown curve; $\Phi_a = 0.5\Phi_0$ for the yellow curve. The drive power reaching the input port of CWR P_{in} was -85 dBm.

The static flux-scan measurements under different drive power of the CWR P_{in} were systematically performed, as shown in the Fig. 8 and 9. The flux of Φ_0 in the SQUID loop corresponded to the dc biased current of 1.4 mA through the coplanar coil.

Figure 8 shows that the resonant frequency $\omega_s / 2\pi$ exhibited a hysteresis with scanning the flux in two different directions (up and down), when the drive power P_{in} was relatively low. With increasing the drive power P_{in} the hysteresis decreased gradually and disappeared eventually at the high enough drive power (shown in Fig. 9(a)). If we increased the drive power P_{in} further, the junctions in the SQUID must

have been overheated, as shown in Fig. 9(b).

With increasing the flux (below Φ_0), the critical current of the SQUID I_c decreased and thus the Josephson inductance of SQUID increased. Therefore, the resonant frequency of CWR $\omega_s / 2\pi$ shifted to lower values (Fig. 8 and 9). However, the hysteretic effect in the flux scan, as shown in the Fig. 8, appears still rather interesting for further discussion.
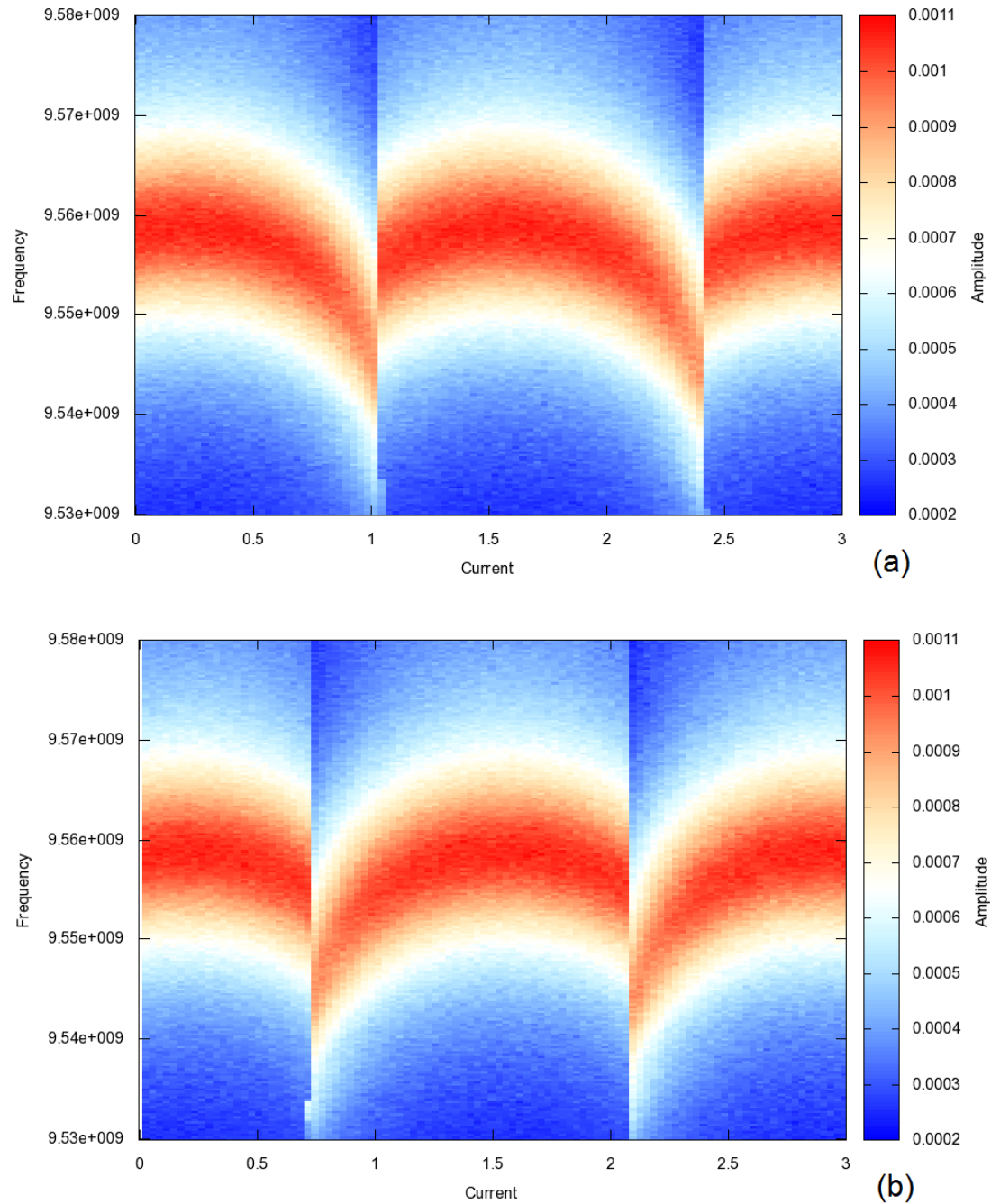
Figure 8. The output response of CWR on the single SQUID sample with scanning the dc biased current for modulating the flux through the SQUID loop. The drive power reaching the CWR P_{in} was -80 dBm. (a) the biased current sweeping up; (b) the biased current sweeping down.
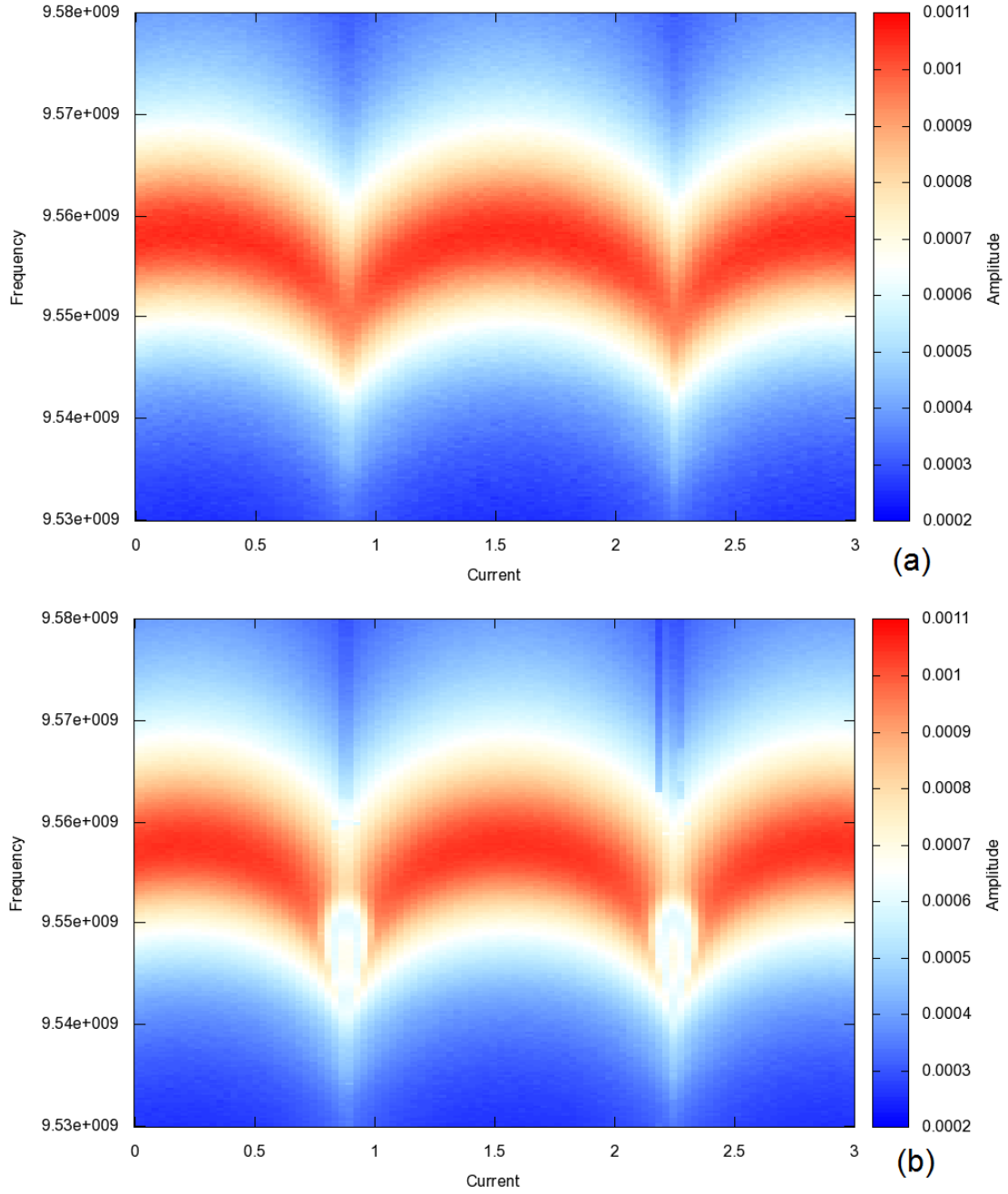
Figure 9. The output response of CWR on the single SQUID sample with scanning the dc biased current for modulating the flux through the SQUID loop. The drive powers reaching the CWR P_{in} were -72 dBm for (a) and -70 for (b), respectively.

According to the discussion in the above theoretical part, under condition that ω_d is much less than ω_{cut} and ω_c, changes of RF flux Φ_{rf} in the SQUID loop can be considered to be adiabatic. The Eq. (15) can then be rewritten as

$$\beta_{rf}\sin\varphi_2 + 2\varphi_2 = \frac{2\pi}{\Phi_0}(\Phi_a + \Phi_d) \tag{19}$$

where $\beta_{\mathrm{rf}} = 2\pi L I_0/\Phi_0$ is the so called SQUID hysteresis parameter [1], and Φ_{a} the static flux introduced by the flux scan. At $\beta_{\mathrm{rf}} < 1$, the potential of the SQUID has one minimum, corresponding to the only stable state. At $\beta_{\mathrm{rf}} > 1$, in addition, there can be several metastable states. For the phase of junction in the SQUID φ_i ($i = 1, 2$), it will exhibit hysteresis with the static flux scan at $\beta_{\mathrm{rf}} > 1$ [1].

Therefore, when the Φ_{d} is tiny compared with the Φ_{a}, the modulation of the φ_i mainly follows the static flux Φ_{a}. The Josephson inductance L_{J} will also display hysteresis with the flux scan, as does also the resonance frequency ω_{s} (shown in Fig. 8). However, when the Φ_{d} is large enough, the function of the SQUID potential v.s. the φ_i will be dramatically modified. The SQUID can switch to another state at $\Phi_{\mathrm{a}} = \Phi_0/2$, and there will be no hysteresis as shown in Fig.9.

Considering the applications of parametric amplifiers, the hysteresis should be eliminated. Hence, the β_{rf} should be made less than one in the further sample designs.

We have also investigated the resonant response of CWR ω_{s} in the two-cell sample (see Fig. 5(b)) as a function of magnetic flux. The resonance frequency ω_{s} was around 10.15 GHz and the modulation of the ω_{s} was found even smaller, about 4 MHz, as shown in Fig. 10. It can be suspected that some junctions of this SQUID had physical defects.
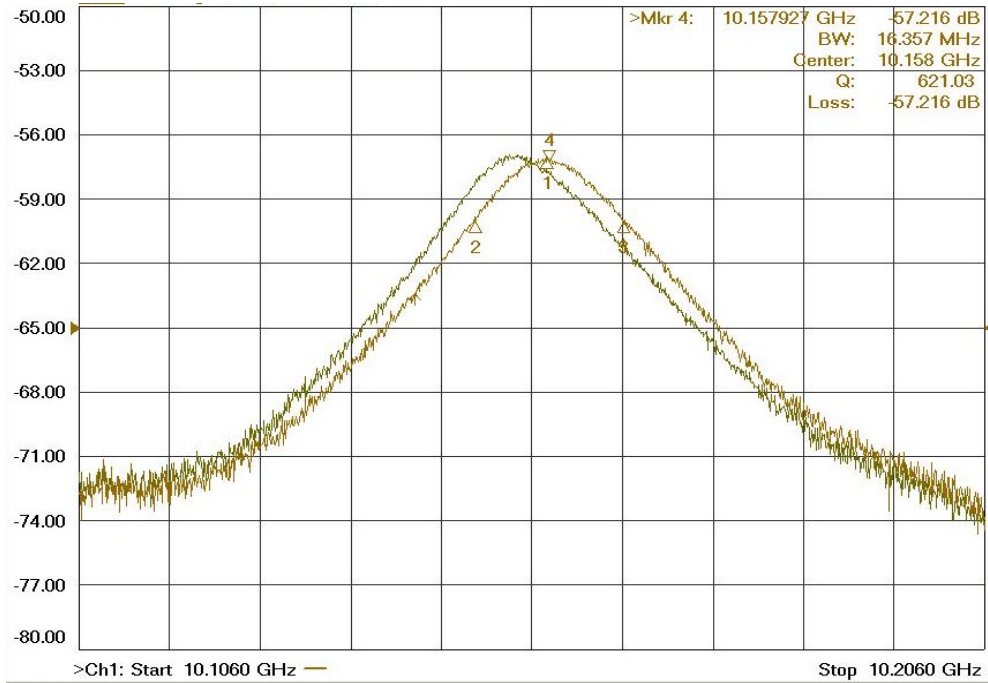

Figure 10. The resonant response of CWR on the two-cell sample with static flux modulation.

3.2 PJBA measurements

To operate the embedded SQUID as a PJBA, the nonlinear regime should be confirmed first. With increasing the drive power of CWR P_{in} on the single SQUID sample, the resonant frequency ω_{s} shifts noticeably to lower frequencies at the drive

power P_{in} = -70 dBm, when the static flux $\Phi_a = 0$. The frequency ω_s reaches its minimum value around P_{in} = -63.5 dBm, as shown in Fig. 11. At even higher drive power P_{in}, the SQUID is already overheated. Based on the discussion in the theoretical part, we conclude that this particular sample displays nonlinear regime but could not reach the bifurcation regime. The sample works in the nonlinear regime in the P_{in} range from -70 dBm to -63.5 dBm at $\Phi_a = 0$.

The shifting range of the ω_s was very small, around 4 MHz (from 9.557 GHz to 9.553 GHz) due to the relatively large critical current of junction I_0 in the SQUID and the large β_L. Therefore the phase changing with different P_{in} was also very small at a fixed frequency around the ω_s, about 20 degrees (shown in Fig. 11). This suggests that the response sensitivity of our sample to the phase difference between the pump and the drive was too low to employ it in RF directional sensor based the PJBA. As for the two-cell sample, the sensitivity was even less.
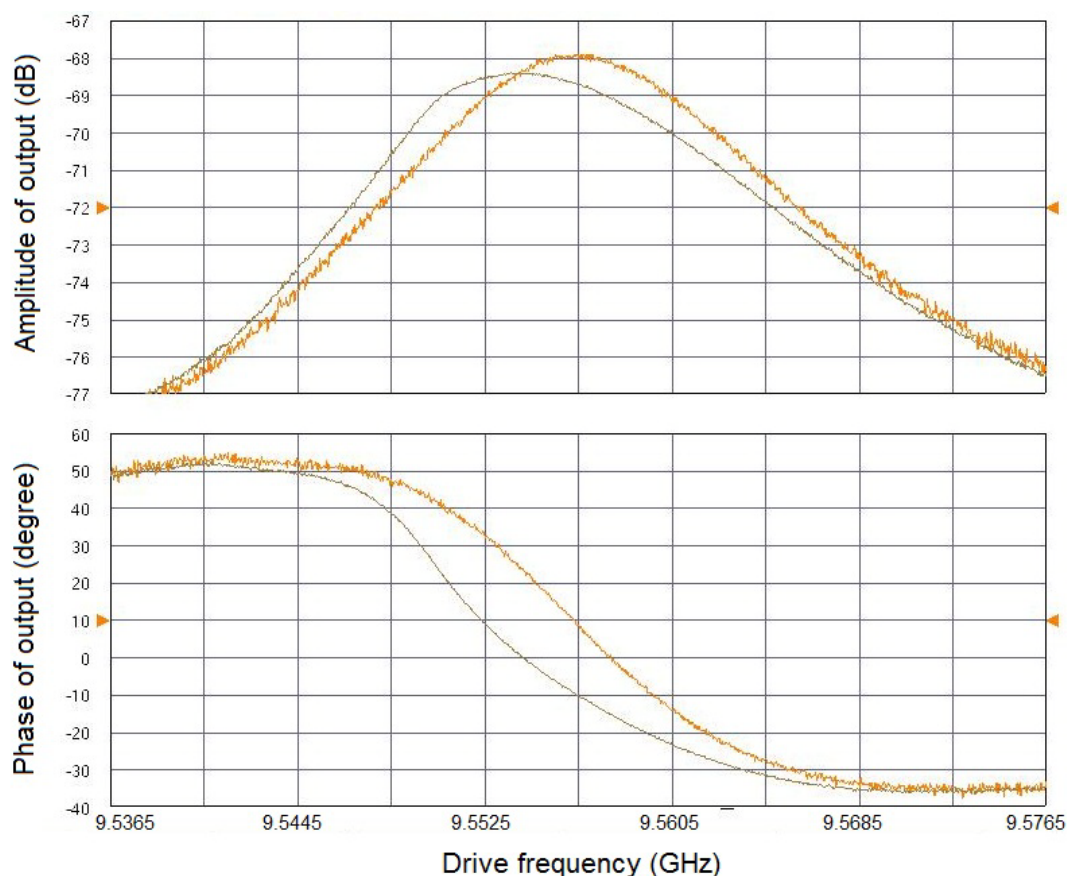
Figure 11. The single SQUID sample working in the nonlinear regime. The drive power P_{in} increased from -70 dBm (yellow curve) to -63.5 dBm (brown curve) at $\Phi_a = 0$.

3.3 AJPA measurements

To operate the embedded SQUID as an AJPA, the RF drive of CWR was set to be around the fundamental resonance frequency $\omega_d = \omega_s$. While two separated RF pumps at the double $\omega_p = 2\omega_d$ with phase difference δ were applied through the two coplanar

coils on the both sides of the SQUID, respectively. Thus the mixed signal at frequency $\omega_m = \omega_p - \omega_d = \omega_d$, which was also near to the resonant frequency ω_s, would be effectively amplified. According to the discussion in the theoretical part, the output amplitude of CWR at frequency ω_d should represent the phase difference between the pump and the drive. It is also easy to show that the output amplitude should reveal the phase difference δ as well. Therefore, this kind of sample could serve as an RF phase-sensitive sensor for the two separated RF pumps and thus provide the basis for the RF directional sensor.

3.3.1 Basic characteristics

The single SQUID sample was studied first to investigate the basic characteristics of AJPA. In this case, RF drive at frequency ω_d = 9.557 GHz and only one RF pump at frequency ω_p = 19.114 GHz were applied. The drive power P_{in} was about -93 dBm; the pump power was chosen relatively high -50 dBm. The amplification gain, which was defined as the difference between the output amplitudes of CWR with and without the pump, was depending on the phase difference between the pump and the drive as shown in Fig. 12.
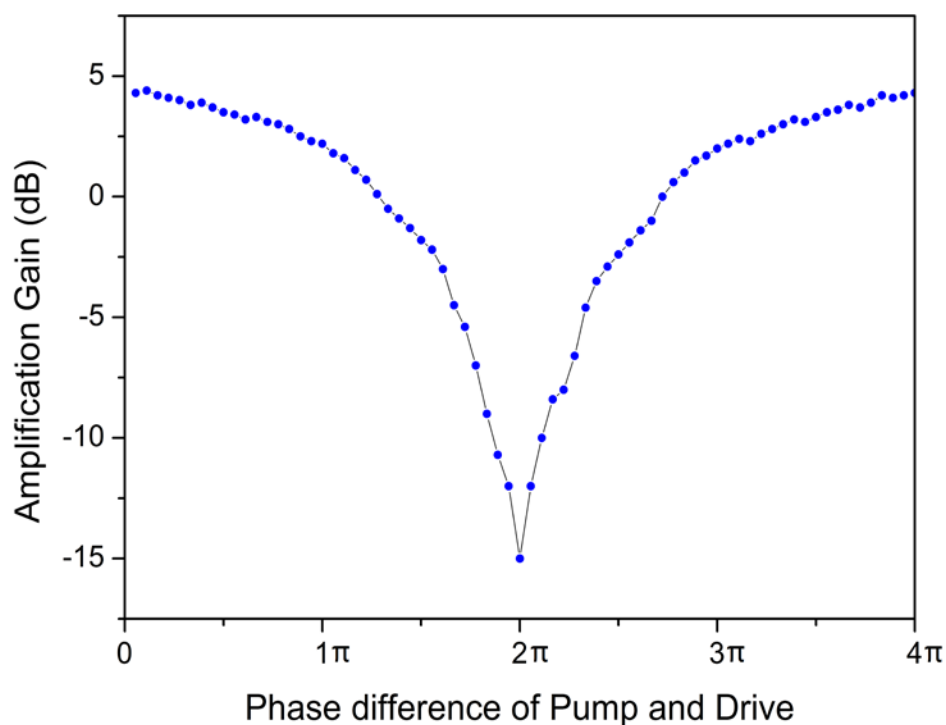
Figure 12. Gain as a function of the phase difference between the RF drive and the pump.

As shown in Fig. 12, the deamplification effect is observed, which is the remarkable characteristic of the AJPA. Since the phase difference of separated RF sources cannot be locked stably, there were fluctuations in the measurement curve. For this configuration, the period of the amplification gain depending on the modulation of the phase of pump was 4π. However, if we modulate the phase of the

drive, the period changes into 2π, as to be expected due to $\omega_d = \omega_p/2$.

We also studied the response of two-cell SQUID device. We did not observe any effect of the pump on the output of CWR. Presumably, there were some defects in the SQUID. Further investigations should be done with new samples later.

3.3.2 Application to RF directional sensor

While two separate RF pumps at the double $\omega_p = 2\omega_d$ with phase difference δ between them were applied, the amplification gain was measured again as a function of one of δ. As shown in Fig. 13, the measured period was 4π as well, which indicates that the two separated RF pumps first mixed with the drive and then combined together. In some range of the period, the sensitivity was relatively high, about 1.2 dB / rad. This, in principle, demonstrates that this kind of sample can be employed as the RF phase-sensitive sensor, which in turn can be used for RF directional detection.
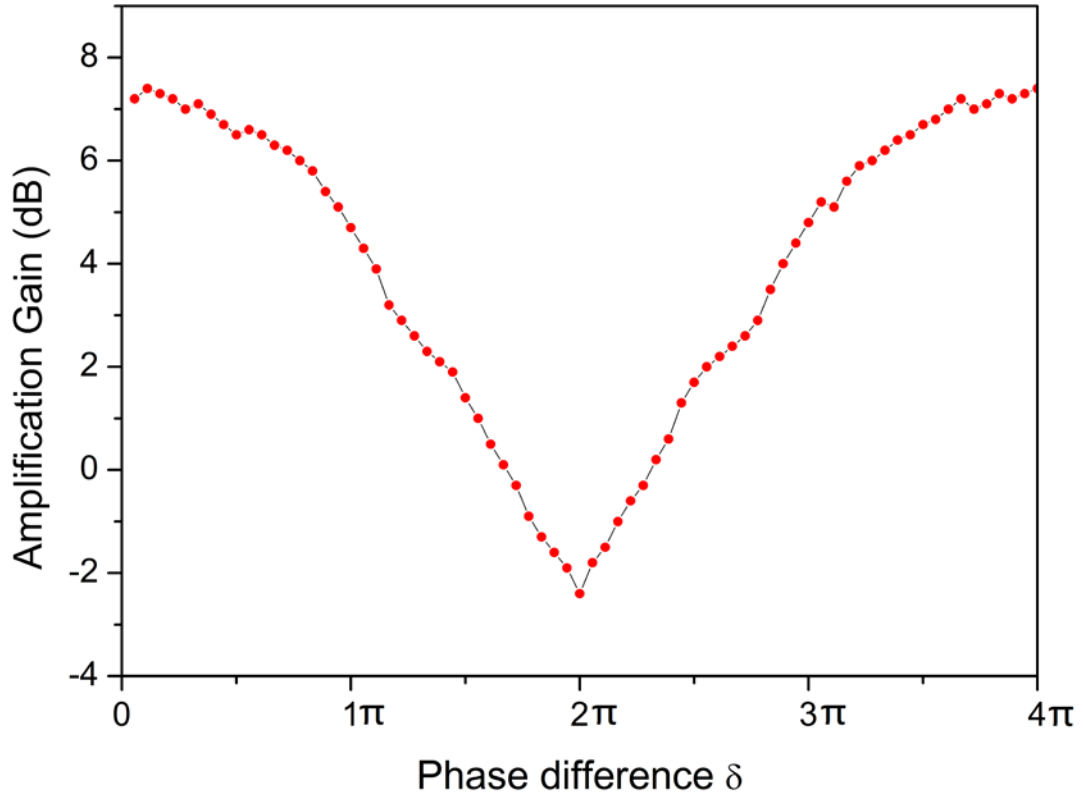
Figure 13. Amplification gain as a function of the phase difference between the two RF pumps.

Conclusion and Outlook

We have studied the response of CPW devices employing single-cell SQUIDs and two-cell SQUIDs with the ultimate goal to develop an RF directional sensor. The operation of such device should be based on the theory of Josephson parametric amplifiers, which we briefly reviewed in the beginning of this report. Our two-cell SQUID sample did not show the expected performance. We suspect that there were some defects in the SQUIDs of present samples. Nevertheless, the single-cell SQUID sample was successfully demonstrated operating as RF phase-sensitive sensor, with sensitivity of 1.2 dB / rad. The relatively large critical current of SQUID I_c limited the nonlinear effects in the Josephson junction, and thus the sensitivity of our sensor.

Hence, in the following works, the critical currents of junctions I_0 in the SQUID should be decreased, so that the corresponding Josephson inductance could be made comparable with the inductance of the coplanar waveguide. The inductance of the SQUID loop should be decreased as well. In this case, the flux-modulation of the I_c should provide more room for choosing bias point of the parametric amplifier. The hysteresis effect with respect to the flux sweep direction will be eliminated, which would make it more convenient for practical operation.

References

[1]   Clarke J and Braginski A 2004 *The SQUID Handbook: Fundamentals and Technology of SQUIDs and SQUID Systems*: Wiley-VCH)

[2]   Michael M and Robert M 2010 Radio-frequency amplifiers based on dc SQUIDs *Superconductor Science and Technology* **23** 093001

[3]   Zimmer H 1967 Parametric amplification of microwaves in superconducting josephson tunnel junctions *Applied Physics Letters* **10** 193-5

[4]   Kanter H and Silver A H 1971 Self-Pumped Josephson Parametric Amplification *Applied Physics Letters* **19** 515-7

[5]   Castellanos-Beltran M A and Lehnert K W 2007 Widely tunable parametric amplifier based on a superconducting quantum interference device array resonator *Applied Physics Letters* **91** 083509-3

[6]   Yamamoto T, Inomata K, Watanabe M, Matsuba K, Miyazaki T, Oliver W D, Nakamura Y and Tsai J S 2008 Flux-driven Josephson parametric amplifier *Applied Physics Letters* **93** 042510-3

[7]   Vijay R, Devoret M H and Siddiqi I 2009 Invited Review Article: The Josephson bifurcation amplifier *Rev Sci Instrum* **80** - 111101

[8]   Bergeal N, Schackert F, Metcalfe M, Vijay R, Manucharyan V E, Frunzio L, Prober D E, Schoelkopf R J, Girvin S M and Devoret M H 2010 Phase-preserving amplification near the quantum limit with a Josephson ring modulator *Nature* **465** 64-8

[9]   Vijay R, Slichter D H and Siddiqi I 2011 Observation of Quantum Jumps in a Superconducting Artificial Atom *Physical Review Letters* **106** 110502

[10]   Siddiqi I, Vijay R, Pierre F, Wilson C M, Metcalfe M, Rigetti C, Frunzio L and Devoret M H 2004 RF-Driven Josephson Bifurcation Amplifier for Quantum Measurement *Physical Review Letters* **93** 207002

[11]   Sage J M, Bolkhovsky V, Oliver W D, Turek B and Welander P B 2011 Study of loss in superconducting coplanar waveguide resonators *Journal of Applied Physics* **109** 063915-10

[12]   Goppl M, Fragner A, Baur M, Bianchetti R, Filipp S, Fink J M, Leek P J, Puebla G, Steffen L and Wallraff A 2008 Coplanar waveguide resonators for circuit quantum electrodynamics *Journal of Applied Physics* **104** 113904-8

[13]   Hatridge M, Vijay R, Slichter D H, Clarke J and Siddiqi I 2011 Dispersive magnetometry with a quantum limited SQUID parametric amplifier *Physical Review B* **83** 134501

[14]   Silver A H and Zimmerman J E 1967 Multiple quantum resonance spectroscopy through weakly connected superconductors *Applied Physics Letters* **10** 142-5

[15]   Werthamer N R and Shapiro S 1967 Analog-Computer Studies of Josephson Radiation Effects *Physical Review* 164 523